EARTH OBSERVATION AND GEOMATICS ENGINEERING
website: https://eoge.ut.ac.ir

Fast extraction of power lines from mobile LiDAR point clouds based on SVM classification in non-urban area

Danesh Shokri[1], Heidar Rastiveis[1]*, Seyed Mohammad Sheikholeslami[2], Reza Shah-Hosseini[1], Jonathan Li[3]

[1]Department of Photogrammetry and Remote Sensing, School of Surveying and Geospatial Eng., University of Tehran, Tehran, Iran
[2]Department of Communications, School of Electrical and Computer Eng., Faculty of Eng., University of Tehran, Tehran, Iran
[3]Department of Geography and Environmental Management, University of Waterloo, Waterloo, Ontario, Canada

Article history:
Received: 12 April 2020, Received in revised form: 15 August 2021, Accepted: 22 August 2021

ABSTRACT

Mobile Laser Scanning (MLS) systems have been used for power line inspection in a fast and precise fashion. However, manually processing of huge LiDAR point clouds is tedious and time-consuming. Thus, an automated method is needed. This study proposes a machine learning-based method for automated detection of power lines from MLS point clouds. The proposed method consists of three main steps: pre-processing, line extraction using Support Vector Machine (SVM), and post-extraction. In the pre-processing step, noisy and low-height points are eliminated after sectioning the collected point clouds. This step considerably reduces the volume of point clouds by 90%. Then, the point features including linearity, planarity, verticality, and the largest component of Principal Component Analysis (PCA) are used as the best-fitted descriptors for power line detection. After training the SVM by a small section of points, SVM properly classified the point clouds with about 97% and 98% accuracies regarding precision and recall, respectively. In the final step, a post-extraction is required to eliminate false points in the power line class. This step improved the recall from 98% to 99.4% and decreased slightly the precision accuracy from 97% to 95.5%. The results demonstrated that the proposed method works rapidly, about 14 seconds per section with an average of 5 million points in each section.

KEYWORDS

Mobile Laser Scanner (MLS)
Point Clouds
Support Vector Machines (SVM)
Powerline Extraction
Cables

1. Introduction

The Light Detection and Ranging (LiDAR) point cloud has become popular in numerous studies, ranging from autonomous driving to urban planning (Grubesic & Nelson, 2020; Li et al., 2019; Shi et al., 2020; Wu et al., 2019). This comes from the fact that LiDAR provides densely 3D information from the surrounding, and more importantly, it can be recorded properly in various illumination conditions (Che et al., 2019; Khodaverdi et al., 2019). Among the three most commonly available LiDAR platforms such as Airborne Laser Scanner (ALS), Mobile Laser Scanner (MLS), or Terrestrial Laser Scanner (TLS), the MLS system has been used vastly in the monitoring of roadside objects including power lines (Biasotto & Kindel, 2018). As shown in Figure 1, a typical MLS system consists of the Global Navigation Satellite System (GNSS), Inertial Measurement Unit (IMU), laser scanners, optical cameras, and Distance Measuring Instruments (DMI), which are integrated and mounted on a vehicle (Nguyen et al., 2018). One main advantage of the MLS compared to the other groups of ALS and TLS is recording the vehicle positioning using the DMI device (trajectory data) (Shokri et al., 2019). This data would play a vital role in the reduction of computational time since it is capable of slicing the large-volume point cloud into smaller sections with the same length (Jung et al., 2019). In terms of collecting datasets, the output of this system is both densely 3D point clouds and high-resolution images of a roadway.

In recent years, both point clouds and color images acquired by an MLS system have been used widely for many purposes such as traffic sign detection, lane marking extraction, pole-like object and car detection, etc. (Liu et al., 2019; R. Liu et al., 2020; Rastiveis et al., 2020; Wu et al., 2020). The main advantage of the MLS system over other systems is that it has a side-view look, and notably near to objects, hence it can record more details related to the objects

* Corresponding author
E-mail addresses: hrasti@ut.ac.ir
DOI: 10.22059/eoge.2022.317348.1092

(Matikainen et al., 2016; Shokri et al., 2021). For instance, traffic sign elements like signboards and pipe signs are detectable in whether the images or the point cloud, whereas they are hardly detectable from an airborne laser scanning (ALS) system (Z. Liu et al., 2020). It should be noted that road accessibility in mountainous areas is a big problem in using vehicle-based MLS systems for powerline monitoring that can be handled by using backpack LiDAR.

Figure 1. Devices mounted on the MLS system (Che et al., 2019)

Powerline agencies have a deep desire to use the MLS datasets, particularly the point cloud, to monitor power lines. This comes from the fact that they cannot only obtain the true location of the utility lines but also analyze the safety situation of the power lines. For this purpose, even though captured images have a lower volume than the point cloud, they have a less applicable in power line monitoring since they are sensitive to the illumination changes, time of the collecting data, viewpoint, and distance of the power lines from the MLS system (Guan et al., 2020). Notably, for getting 3d information from the images, a land surveying process is required, however, this is tedious and time-consuming (Matikainen et al., 2016). On the other hand, the point cloud not only excludes such image drawbacks but also provides more precise information about the cables or the poles. As can be seen from Table 1, which shows a comparison between the LiDAR and Image systems, the LiDAR systems provide dense 3D points from a side view look with high precision, but it is comparably more expensive than the image platforms.

This study aims to propose a fast and automated process for extracting distribution power lines from the MLS point cloud based on the Support Vector Machine (SVM) algorithm which is the key contribution of this paper. In addition, this method suggests a robust pre-processing step for eliminating unneeded points which enhances the time of implementation criteria and overcomes the immense volume of the MLS point cloud. Noticeably, the algorithm not only shows insensitivity to the size, position, and illumination changes of the cables but also non-cable objects such as densely trees and cars have no negative influence on the results. This means that the algorithm works in complex environments.

Table 1. Comparison of image and LiDAR systems.

	Data	Illumination	Processing	Scale	Density	Precision	Volume	Cost
LiDAR Point Clouds	3D	Not Sensitive	Fast	Fixed	High	High	High	High
2D Image	2D	Sensitive	Slow	Variable	Low	Low	Low	Low

2. Literature Review

Methods of power line monitoring from the LiDAR point cloud can be categorized into two classes: mathematical estimation and machine learning-based methods. Regarding the mathematical estimation approaches, researchers generally used the line extraction algorithms such as the Hough Transform (HT) algorithm for power line detection (Matikainen et al., 2016; Zhu & Hyyppä, 2014a). This may be because cables follow a linearity state from the top view that with help of these line extraction methods their vicinity can be estimated. For example, Guan et al. (2016) extracted both elements of poles and cables belonging to the power lines. They firstly filtered the collected point cloud by both the trajectory data and the elevation of the vehicle. Then, the cables were extracted by the HT, and afterward, modeled by a 3D fitting process. Similarly, Yadav and Chousalkar (2017) detected only the cables located in the urban, peri-urban, and rural sites. They applied elevation filters for eliminating unneeded points and reduction in the volume of the datasets. Then, a density-based approach was proposed to remove trees and building objects. Finally, they detected and modeled available cables using the HT and a second-order polynomial equation respectively with more than 90.84% completeness accuracy. Regarding utility poles, many studies have been done on the pole-like objects extraction including utility poles (Kang et al., 2018; Li et al., 2016; R. Liu et al., 2020). The most common algorithms used in these kinds of studies are Principle Component Analysis (PCA) and 3D voxels.

These mathematical-based algorithms work rarely in a small section where the linearity of the cables is not a distinguished parameter (Ma, 2020). Notably, if the objects like trees and buildings are not eliminated, they are unable to extract the cables properly (Wang et al., 2019). Thus, machine-learning procedures were introduced for power line investigation because they are capable of using the linearity and other attributes of the cables such as elevation and verticality simultaneously. For example, Wang et al. (2017) proposed a Radial Basis Function (RBF)-SVM method for power line extraction. Different methods of neighborhood selection points such as multi-scale slant cylindrical were used for calculating the descriptors of linearity and scattering. They acquired 97% accuracy in the quality rate of the power line classification. Likewise, urban objects including power lines were classified by the SVM method in the study of Zhang et al. (2013). Geometry, radiometry, topology and echo characteristics were the considered features during the classification. They gained 86% kappa coefficient for converting the collected point cloud to labels of ground, building, vegetation, power lines and trees.

In the last decade, voxel-based procedures have gained popularity in power line cables extraction because of having fixed size and discrete coordinates. Jung et al. (2020) proposed a hierarchical approach for power line detection with help of voxels and machine learning descriptors such as linearity and planarity. This algorithm acquired an accuracy range between 88.87% and 95.47% in the MLS point cloud. Likewise, Shokri et al. (2021) suggested a voxel and mathematical-based approach for detecting both cables and poles. They initially estimated the location of power line poles by HT algorithm, where cables were segmented by considering voxel processing between every two adjacent poles. This method was tested on three MLS data in urban and non-urban environments which gained an accuracy of about 95%. In a novelty way, an Entropy-Weighting Method (EWM) was proposed by Tan et al. (2021) study to classify transmission power lines and a 98% accuracy was reported.

Even though the previous works have detected power lines with various algorithms ranging from mathematical-based ones to deep neural network structures, there are some gaps in power line monitoring. For example, a few studies have focused on the distribution lines, as the most common power lines which carry low voltage of electricity. For analyzing the performance of previous works, four criteria play a key role in discussing; (i) time of implementation, (ii) used parameters and thresholds, (iii) accuracy, and (iv) type of extracted power lines – distribution or transmission lines which carry respectively low and high voltages of electricity. Studies like Shi et al. (2020); Shokri et al. (2021); Tan et al. (2021) represented mathematical approaches such as HT, and Random Sample Consensus (RANSAC) for power line extraction acquired acceptable results for both distribution and transmission lines. However, these methods have used numerous parameters with fixed thresholds that need to be tuned for a new dataset. Also, converting the 3D point cloud into a two-dimensional feature space was another drawback of these works. Additionally, using massive training data and time consuming were two considerable disadvantages of deep learning-based frameworks.

3. Method

As shown in Figure 2, the proposed algorithm is composed of three consecutive steps including pre-processing, cables classification, and post extraction.

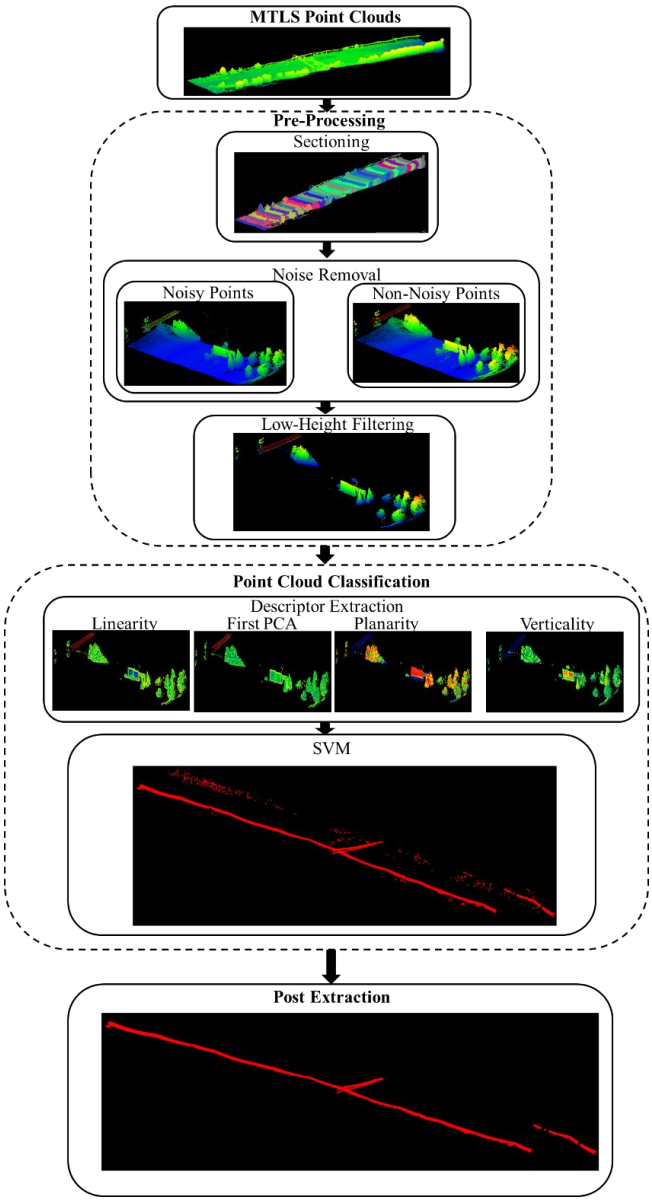

Figure 2. Flowchart of the proposed algorithm.

3.1. Pre-processing

This step aims to divide the collected point cloud into many equal-length sections in addition to removing noisy and unneeded points which includes three main tasks.

3.1.1. Sectioning

As shown in Figure 3, the trajectory data gives information about the vehicle position. This information can be used for partitioning the collected point cloud into several equal-length tiles to speed up the computation time. In terms of the sectioning length, researchers generally select it based on their computing systems and focused area (Lehtomäki et al., 2019). But in this study, we choose the length of each section based on the average velocity of the vehicle per second. This means that if we consider the time as one second, the sectioning length (L), would be equal to the average velocity (V) based on the Equation (1):

$$L = \frac{\sum_{i=1}^{n} V_i}{n} \quad (1)$$

where n is the number of recorded velocities for the MLS system. If the final time of power line detection is less than one second, the proposed algorithm can be used in real-time situations. Since power lines follow a lengthy shape structure, locating a cable between two adjacent sections would not affect the results. Therefore, there is no need to consider overlaps between adjacent sections.

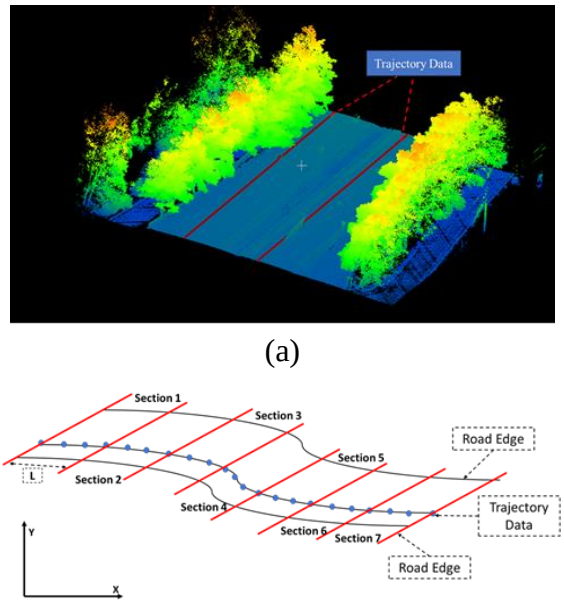

Figure 3. Sectioning the collected point cloud to small same-length tiles; (a) Displaying the trajectory data on a sample collected point cloud; (b) Schematically drawing the process of sectioning (Shokri et al., 2019)

3.1.2. Noise Removal

Since the MLS system consists of several integrated pieces of equipment such as GPS and IMU, errors related to the sensors and system integration can be occurred during collecting the point cloud (Xu et al., 2015). Therefore, the error is categorized into two classes: (i) elevation-based and (ii) distance-based errors.

The elevation-based error means there are some available types of points, which have abnormal elevation. The main cause of these errors is the high-height objects like trees and buildings because they cause the multipath effect on the GPS. To correct these blunders, we use the mean (μ) and standard deviation (σ) to detect these errors proposed in Shokri et al. (2019) (Equations 2 and 3).

$$\mu = \frac{\sum_{i=1}^{k} Z_i}{k} \quad (2)$$

$$\sigma = \frac{\sum_{i=1}^{k} (Z_i - \mu)^2}{k} \quad (3)$$

Where Z is the elevation of neighborhood points and k is the number of points in the neighborhood region.

Here, to accelerate the process, the search area is reduced by limiting it to higher elevation points. the only needed parameter is the spherical radius which extracts the points located in a specific neighborhood radius of each point (Wang et al., 2019). The optimized value of it was acquired based on a trial-and-test procedure, and the sensitivity analysis of this parameter is further discussed in chapter 5.

Regarding the distance-based errors, it can be mentioned that as long as the distance of objects increases from the MLS vehicle, the errors are increased (see Figure 4). This exists for any MLS platform because of the system integration, and notably is about 3 cm (Di Stefano et al., 2021). Since machine learning methods such as SVM are based on features and neighborhood points, the noisy points are removed before the classification step. Consequently, thanks to the trajectory data, we apply a width threshold on each section to limit the data range. For applying the width parameter on each point cloud section, the distance of each point is perpendicularly calculated from the trajectory data on XY coordinate system. If it is more than the width threshold, it would be considered a noisy point and is eliminated. The optimized value of the width threshold is discussed in the Discussion section in terms of computation time and acquired accuracies.

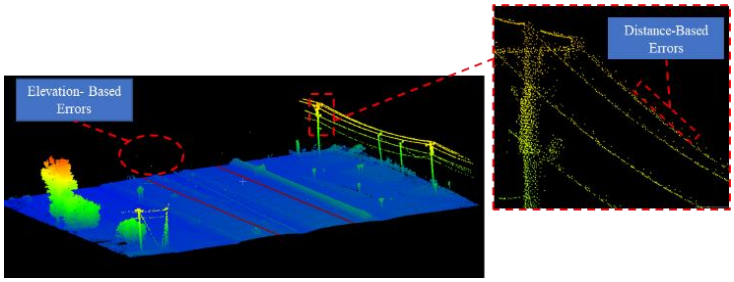

Figure 4. Displaying the distance- and elevation-based errors.

3.1.3. Low-height Filtering

Based on Guan et al. (2016) study, the minimum elevation of power line cables from the ground is about 5m in the USA. This intrinsic feature of power lines can play a key role in removing unneeded points because the elevation of the cables is much higher than the altitude of the MLS vehicle over the world. Therefore, points whose elevation is lower than the MLS vehicle altitude from the ground surface are considered unneeded points and are eliminated from the data. This would considerably enhance the computation time due to removing a significant number of non-power line points.

3.2. Point cloud classification

Descriptor extraction and semantic labeling are two common steps for point cloud classification which we discuss as follows;

3.2.1. Descriptor Extraction

The point cloud is irregular and cannot be used solely in the process of classification. Therefore, researchers use features such as geometry and radiometric features for information extraction from point cloud data (Xia et al., 2020). Then, these extracted features are fed to the classification methods. In this research, among numerous features, we used linearity, planarity, verticality and lastly the largest normalized eigenvalue of Principal Component Analysis (PCA), as the best-fitted descriptors for MLS point cloud classification which are suggested in Zaboli et al. (2019). One common attribute of these selected features is that all of them are calculated from the PCA. The process of calculating these features consists of three steps. Firstly, for each point, their neighborhood points located in a sphere are selected. Afterward, the normalized eigenvalues of PCA (e_1, e_2, e_3) and also eigenvectors (E_1, E_2, E_3) are measured which $e_1 > e_2 > e_3$ (Equation 4) (Levada, 2020). The normal vector of a plane (n_z) is another acquired parameter by PCA which needed in the verticality descriptor. Then, based on these PCA components, considered features are acquired as follow:

$$A = [E_1 \quad E_2 \quad E_3] \begin{bmatrix} e_1 & 0 & 0 \\ 0 & e_2 & 0 \\ 0 & 0 & e_3 \end{bmatrix} [E_1 \quad E_2 \quad E_2] \tag{4}$$

$$Linearity = \frac{e_1 - e_2}{e_1} \tag{5}$$

$$Planarity = \frac{e_2 - e_3}{e_1} \tag{6}$$

$$Verticality = 1 - n_z \tag{7}$$

3.2.2. Support Vector Machine (SVM) Classification

To detect cables using the selected features, two approaches can be used; (i) supervised and (ii) un-supervised methods. The algorithms based on the trained features (supervised) are mainly accurate and reliable (Papa et al., 2012). This is because of well-known and labeled training input data. SVM is a sample of a supervised algorithm that works based on fitting a hyperplane in the n-dimensional space of the features (Vishwanathan & Narasimha Murty, 2002). It separates the labeled cable and non-cable points using kernel functions. Here the Radial Basis Function (RBF), which is a popular kernel due to its simplicity, was used (Barakat & Bradley, 2010). It should be noted that in this paper the basic theory of the SVM is not discussed and readers are referred to (Vishwanathan & Narasimha Murty, 2002) and (Barakat and Bradley, 2010) for further information.

3.3. Post-processing

To enhance the final output of the proposed algorithm, a Euclidean distance based clustering procedure is suggested to eliminate points that are falsely extracted as the cable class. Therefore, this clustering is implemented on the cable class points which is the final output of the SVM method (Guan et al., 2016). Afterward, the density condition is applied to each cluster, meaning that those segments that have a density of more than 35 points are selected as the true cables; otherwise, non-cable points would be removed. Based on trial-and-error analysis on several point cloud sections, it was observed that several tree points would be wrongly extracted. The main attribute of these points was their low-density value lower than 35 points, while the cables followed a higher density. This is discussed in detail in the Discussion section.

4. Experiment and Results

4.1 Study area

The proposed algorithm was assessed in the MLS point cloud collected along with a non urban environment in Anderson, South Carolina, USA (Shokri et al., 2021). The selected area consists of various challenging objects, ranging from dense trees to numerous cars on the roads. The MLS system records 55 million points for the region with a length of about 650 m (Figure 5).

Due to the huge volume of the collected point cloud (i.e. 1.46 GB), the sectioning step was generated to create low-volume sections. The length of each section was considered based on the moving vehicle distance in each second. As the average velocity of the MLS system was 60 km/h (or 17m/s), the section length obtained was equal to 17 m. It should be noted that we use the trajectory of one side of the road; however, the collected points during the return route are also extracted and processed in each section. Figure 6 displays the created sections with multicolor with an average of 5 million points in each section.

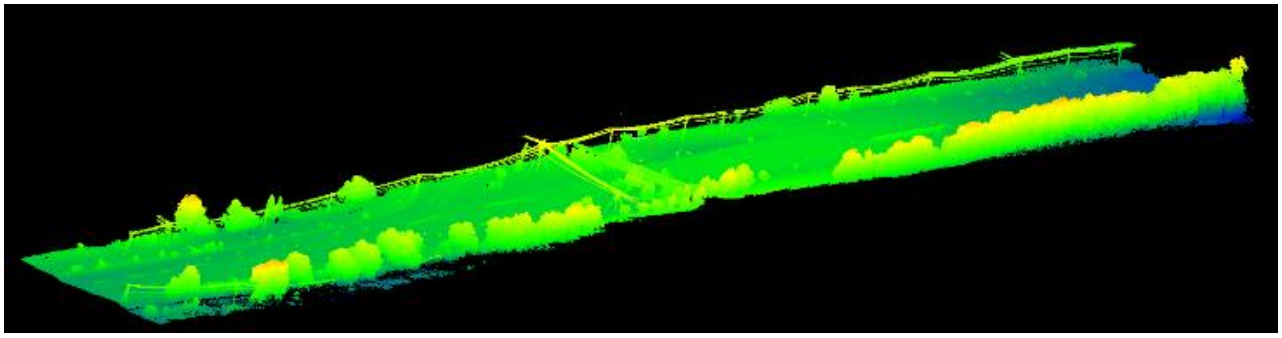

Figure 5. Collecting the point cloud by the MLS system from the non-urban environment.

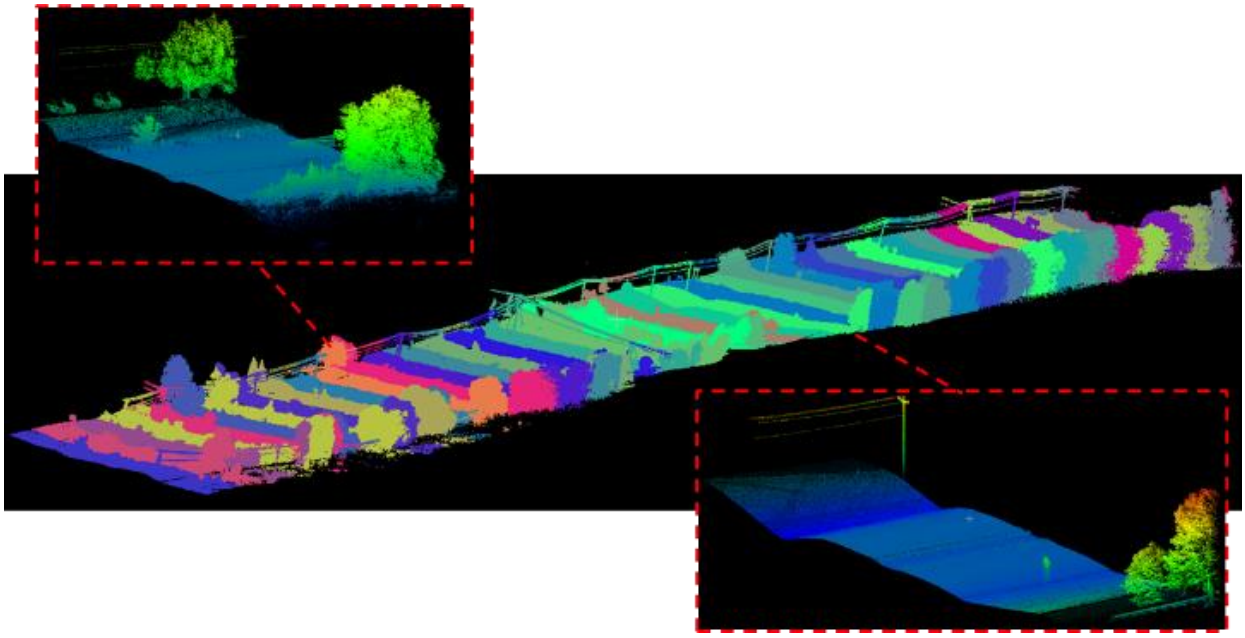

Figure 6. Sectioning the collected point cloud.

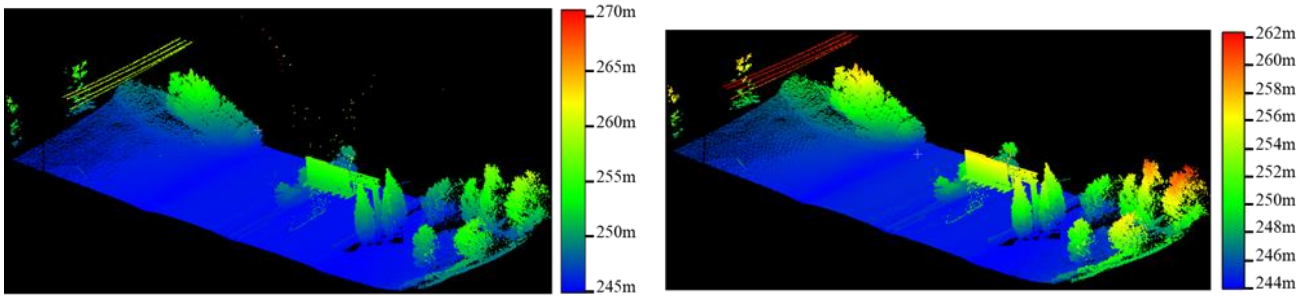

(a) (b)

Figure 7. Eliminating noisy points; (a) a sample noisy section; (b) a non-noise section

4.2. Results

Regarding noisy points, we firstly eliminated the elevation-based errors like our previous study by Shokri et al. (2019), in which the neighborhood points were considered 20. As shown in Figure 7, the maximum elevation reduced significantly from 270 m to about 260 m. Similarly, those objects that had a perpendicular distance of more than 30 m from the trajectory data were removed (distance-based errors).

As shown in Figure 7(b), an extensive amount of collected points belong to the low height objects, particularly the ground surface. So, if they are eliminated, the volume of each section would be considerably reduced. For this purpose, those points had an altitude lower than the elevation of both the MLS vehicle (1.8m), and corresponding trajectory data on the road surface were selected as the low height objects

and removed. As shown in Figure 8, sharply the number of point clouds fall from about 1.2 million to 120 thousand points showing around 90% reduction in the volume.

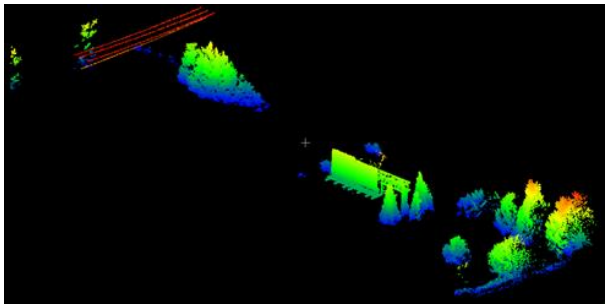

Figure 8. Eliminating the low-height points.

After removing unneeded points, selected features of linearity, planarity, verticality, and the largest component of PCA were extracted. A 0.6 m spherical radius for choosing each neighborhood point was considered based on the Zaboli et al. (2019) study, where the same MLS system was used. As shown in Figure 9, the acquired amount of the linearity and the largest PCA component are near 1, whereas the other two features are close to zero. Also, the histogram of each feature can be seen beside the corresponding descriptor from the Figure 9.

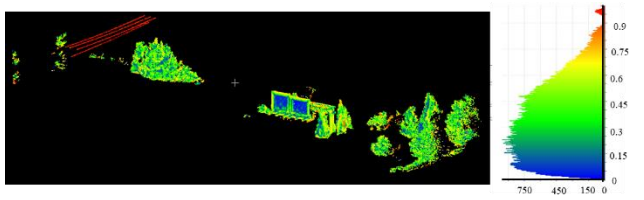

(a)

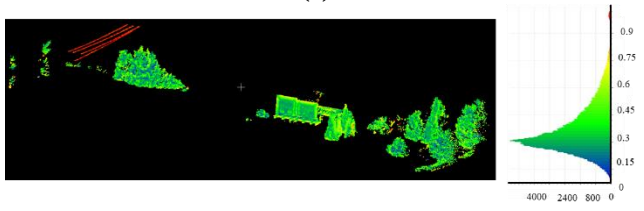

(b)

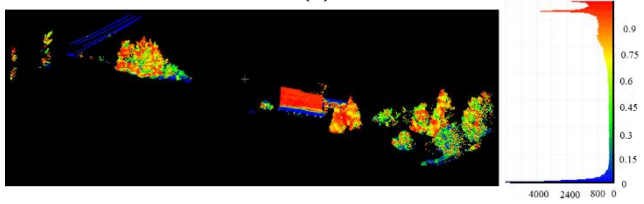

(c)

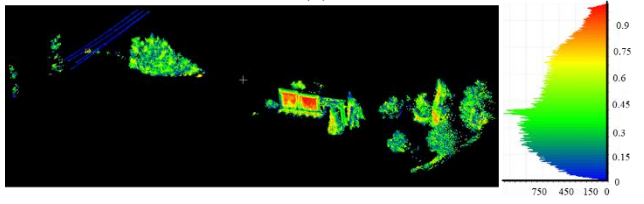

(d)

Figure 9. Descriptor extraction; (a) Linearity; (b) The (d) largest component of PCA; (c) Verticality; (d) Planarity.

Since the SVM classification needs training data, here we selected a few parts of the region as the training section. Figure 10-a gives information about the trained cables with a length of about 32 m and 2300 points. Also, some parts of the poles (see Figure 10(b)), trees (Figure 10(c)), and notably the adjacent part of trees (see Figure 10(d)) were selected for the non-cable labels. The amount of these non-cable points was about 12,000 points.

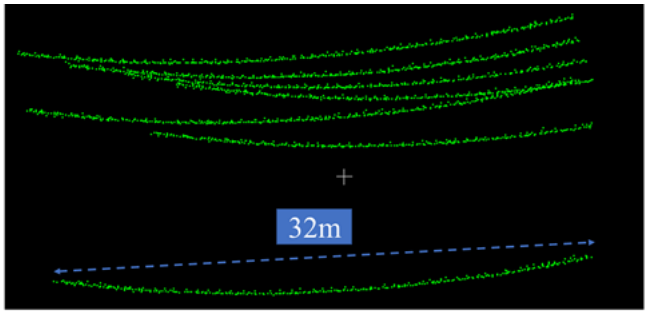

(a)

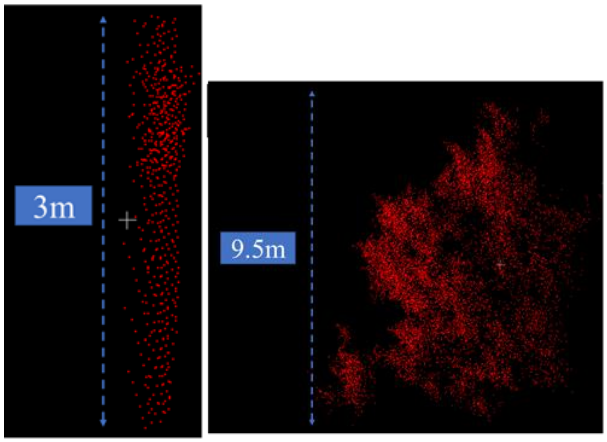

(b) (c)

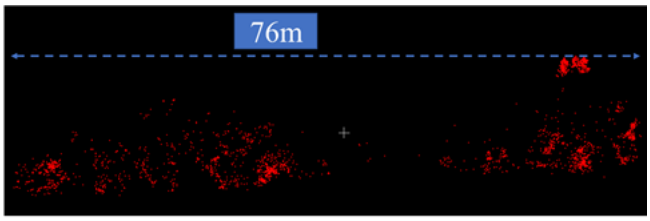

(d)

Figure 10. Training points for the SVM; (a) Cable label; (b) Poles, (c) trees, and (d) adjacent tree points as the non-cable label.

As shown in Figure 11(a), our method can successfully classify the MLS point cloud into the power line and non-power line after training the SVM. Figure 11(a) also shows that a considerable number of tree points were extracted falsely as power lines. Therefore, the power line points were clustered based on the Region Growing algorithm with a 3 m distance threshold. By applying a density limitation (35) on each cluster, significant amounts of false points were removed, see Figure 11(b).

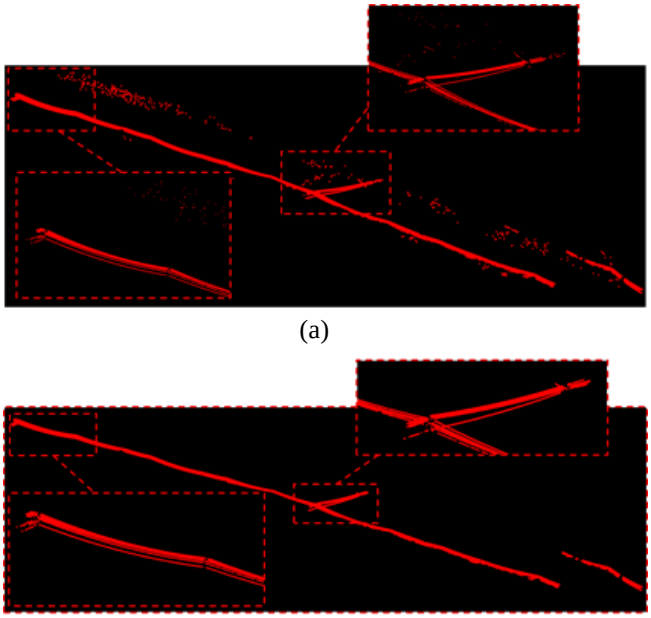

(a)

(b)

Figure 11. Cables detection; (a) Output of the cable class by the SVM; (b) Post-processing for the removing false points;

4.3. Accuracy assessment

The algorithm truly detected 36,701 points among 37,837 points belonging to power lines (True Positive and False Positive). Regarding the false detective, 901 points are considered falsely as the cable points that mainly belonged to the dense trees (False Negative). Based on Equations (8) and (9) (Zaboli et al., 2019), the precision and recall obtained are 97% and 98%, respectively.

$$\text{Precision} = \frac{\text{True Positive}}{\text{True Postive+False Psotive}} \quad (8)$$

$$\text{Recall} = \frac{\text{True Positive}}{\text{True Postive+False Negative}} \quad (9)$$

For enhancing the recall accuracy, after segmenting the cable class, those segments that had a density lower than 35 were removed. This improved the recall accuracy by 1.4 %, increasing from 98.0% to 99.4% because the points belong to trees extracted as the cable, easily removed by applying this density condition. But the precision accuracy decreased slightly from 97.0% to 95.5% because some parts of the wires were eliminated.

5. Discussion

The proposed algorithm is going to be assessed from three aspects; (i) time of implementation, (ii) comparison with other related algorithms, and lastly (iii) parameter optimization.

The programming environment of MATLAB 2015-a was selected for running the proposed algorithm. Also, the computer was a laptop with Intel (R) Core (TM) i5-3210M CPU @2.50GHz, 12GB RAM, DDR 3, NVidia GeForce 2.630 GB. Note, there is no need for any cloud computing system for running the proposed algorithm, unlike other studies (Yadav & Chousalkar, 2017; Yadav et al., 2016). Averagely, each section took about 14 seconds of processing for extracting the power line cables.

In terms of the used parameters, Table 2 indicates the sensitivity analysis of the used parameters with their optimized values. Three criteria of time, precision and recall accuracies have been chosen to evaluate different values. For example, as long as the sectioning length is increased, the processing time is also increased which may be problematic for real-time monitoring. Although the spherical radius was selected based on Zaboli et al. (2019), our sensitivity analysis proved it as the optimized value.

Table 2. Sensitivity analysis of the proposed algorithm parameters.

Steps	Test Variables	Values (m)	Time (Sec)	Average	
				Recall (%)	**Precision (%)**
Pre-Processing	Section Length	10	12.3	99.4	95.5
		17	**14.0**	**99.4**	**95.5**
		20	15.8	99.4	95.5
		30	37.2	99.4	95.5
	Neighbourhood Points	10	12.2	99.4	94.1
		20	**14.0**	**99.4**	**95.5**
		30	16.3	88.3	92.6
		40	21.5	80.2	88.3
	Width Threshold	25	10.5	91.6	98.3
		30	12.2	95.3	97.8
		35	**14.0**	**99.4**	**95.5**
		40	16.3	99.4	95.5
Cable Extraction	Spherical Radius	0.2	11.8	94.7	91.2
		0.6	**14.0**	**99.4**	**95.5**
		1.0	21.5	95.3	95.5
		1.5	27.6	92.2	95.5
Post Processing	Distance Threshold	1	13.3	97.3	95.5
		2	13.6	98.7	95.5
		3	**14.0**	**99.4**	**95.5**
		4	14.1	99.4	94.1
	Density Limitation	30	13.5	99.4	94.3
		35	**14.0**	**99.4**	**95.5**
		40	14.3	96.8	96.3
		45	14.6	93.3	98.7

In comparison with the other state-of-the-art studies, the algorithm is going to be evaluated concerning the time of running, acquired accuracy, supplemental data, used thresholds, and lastly the tested environment. Our algorithm directly consumes the recorded MLS data needless of requiring any conversion between two separate spaces, while

methods of (Guan et al., 2016; Jung et al., 2020; Zhu & Hyyppä, 2014b) need a transformation from the 3D LiDAR point cloud space to a 2D binary image generation. More importantly, the algorithm would not need supplementary data, unlike Husain and Chandra Vaishya (2018) study that used the return number data as an input. Another positive side of our work was extracting power lines in various challengeable objects like densely trees, numerous cars, pole-like objects in various shapes, and so on, while studies (Ortega et al., 2019; Tan et al., 2021) recognized the power line cables just in low challengeable regions including power lines and bushes. Using fewer thresholds was another advantage of our algorithm than previous ones such as (Awrangjeb, 2019; Munir et al., 2021; Yadav & Chousalkar, 2017) which mostly have considered several parameters, in some cases more than 10 parameters. In terms of the acquired accuracies regardless of other parameters, in some cases, our algorithm gained higher accuracies than previous studies. For example, our algorithm gained a recall accuracy near 99% while studies by Tan et al. (2021) at about 98%, Shokri et al. (2021) at 95%, and Awrangjeb (2019), at around 95%.

6. Conclusion

This study proposed a machine learning-based algorithm for extracting power lines from the MLS point cloud. For this purpose, three consecutive steps of pre-processing, power line extraction by SVM, and lastly post extraction were considered. Looking firstly at the pre-processing, more than 90% of unneeded points like noisy and ground points were removed properly. Then, linearity, planarity, verticality, and the largest component of PCA were selected as the best fitting descriptors for cable detection. In the next step, each of which descriptors are extracted for high-height points by considering the neighborhood radios of 0.6 m. Afterward, SVM was trained by a small section that successfully classified the point cloud at about 97% and 98% in both precision and recall respectively. Also, the recall was improved to 99.4% by introducing a segmentation stage for removing non-cable points.

The main advantages of this algorithm can be summarized as; (i) robust in complex environments; (ii) fast and easy implementation and (iii) proposing the best-fitted descriptors. This algorithm can be suggested for extracting different elements of power lines such as utility poles and cross arms. One can use a 2nd order curve as a shape constraint during the cable extraction step to get a higher accuracy that is suggested to be considered in future studies. The only object that harmed the final results was the trees. Therefore, it is suggested that initially detecting and eliminating trees from the point cloud using different methods would be tested and analyzed in future studies.

Acknowledgments

The authors would like to acknowledge Dr. Wayne A. Sarasua at Clemson University and Dr. Alireza Shams at Mercer University for providing the dataset of this research.

References

Awrangjeb, M. (2019). Extraction of Power Line Pylons and Wires Using Airborne LiDAR Data at Different Height Levels. Remote Sensing, 11(15), 1798. https://www.mdpi.com/2072-4292/11/15/1798

Barakat, N., & Bradley, A. P. (2010). Rule extraction from support vector machines: A review. Neurocomputing, 74(1), 178-190. https://doi.org/10.1016/j.neucom.2010.02.016

Biasotto, L. D., & Kindel, A. (2018). Power lines and impacts on biodiversity: A systematic review. Environmental Impact Assessment Review, 71, 110-119. https://doi.org/10.1016/j.eiar.2018.04.010

Che, E., Jung, J., & Olsen, M. J. (2019). Object Recognition, Segmentation, and Classification of Mobile Laser Scanning Point Clouds: A State of the Art Review. sensors, 19(4). https://doi.org/10.3390/s19040810

Di Stefano, F., Chiappini, S., Gorreja, A., Balestra, M., & Pierdicca, R. (2021). Mobile 3D scan LiDAR: a literature review. Geomatics, Natural Hazards and Risk, 12(1), 2387-2429. https://doi.org/10.1080/19475705.2021.1964617

Grubesic, T. H., & Nelson, J. R. (2020). UAS Platforms and Applications for Mapping and Urban Analysis. In T. H. Grubesic & J. R. Nelson (Eds.), UAVs and Urban Spatial Analysis: An Introduction (pp. 13-29). Springer International Publishing. https://doi.org/10.1007/978-3-030-35865-5_2

Guan, H., Yu, Y., Li, J., Ji, Z., & Zhang, Q. (2016). Extraction of power-transmission lines from vehicle-borne lidar data. International Journal of Remote Sensing, 37(1), 229-247. https://doi.org/10.1080/01431161.2015.1125549

Guan, H., Yu, Y., Peng, D., Zang, Y., Lu, J., Li, A., & Li, J. (2020). A Convolutional Capsule Network for Traffic-Sign Recognition Using Mobile LiDAR Data With Digital Images. IEEE Geoscience and Remote Sensing Letters, 17(6), 1067-1071. https://doi.org/10.1109/LGRS.2019.2939354

Husain, A., & Chandra Vaishya, R. (2018). An Automated Method for Power Line Points Detection from Terrestrial LiDAR Data. Emerging Technologies in Data Mining and Information Security, 813, 459-472. https://doi.org/10.1007/978-981-13-1498-8_41

Jung, J., Che, E., Olsen, M. J., & Parrish, C. (2019). Efficient and robust lane marking extraction from mobile lidar point clouds. ISPRS Journal of Photogrammetry and Remote Sensing, 147, 1. https://doi.org/10.1016/j.isprsjprs.2018.11.012

Jung, J., Che, E., Olsen, M. J., & Shafer, K. C. (2020). Automated and efficient powerline extraction from laser scanning data using a voxel-based subsampling with hierarchical approach. ISPRS Journal of Photogrammetry and Remote Sensing, 163, 343-361. https://doi.org/10.1016/j.isprsjprs.2020.03.018

Kang, Z., Yang, J., Zhong, R., Wu, Y., Shi, Z., & Lindenbergh, R. (2018). Voxel-Based Extraction and Classification of 3-D Pole-Like Objects From Mobile LiDAR Point Cloud Data. IEEE Journal of Selected Topics in Applied Earth Observations and Remote Sensing, 11(11), 4287-4298. https://doi.org/10.1109/JSTARS.2018.2869801

Khodaverdi, N., Rastiveis, H., & Jouybari, A. (2019). Combination of post-earthquake LiDAR data and satellite imagery for buildings damage detection. Earth Observation and Geomatics Engineering, 3(1), 12-20. https://dx.doi.org/10.22059/eoge.2019.278307.1046

Lehtomäki, M., Kukko, A., Matikainen, L., Hyyppä, J., Kaartinen, H., & Jaakkola, A. (2019). Power line mapping technique using all-terrain mobile laser scanning. Automation in Construction, 105, 102802. https://doi.org/10.1016/j.autcon.2019.03.023

Levada, A. L. M. (2020). Parametric PCA for unsupervised metric learning. Pattern Recognition Letters, 135, 425-430. https://doi.org/10.1016/j.patrec.2020.05.011

Li, F., Elberink, S. O., & Vosselman, G. (2016, 12–19 July 2016). Pole-Like Street Furniture Decomposion in Mobile Laser Scanning Data [XXIII ISPRS Congress]. ISPRS Annals of the Photogrammetry, Remote Sensing and Spatial Information Sciences, Prague, Czech Republic. https://doi.org/10.5194/isprs-annals-III-3-193-2016

Li, F., Lehtomäki, M., Oude Elberink, S., Vosselman, G., Kukko, A., Puttonen, E., . . . Hyyppä, J. (2019). Semantic segmentation of road furniture in mobile laser scanning data. ISPRS Journal of Photogrammetry and Remote Sensing, 154, 98-113. https://doi.org/10.1016/j.isprsjprs.2019.06.001

Liu, C., Li, S., Chang, F., & Wang, Y. (2019). Machine Vision Based Traffic Sign Detection Methods: Review, Analyses and Perspectives. IEEE Access, 7, 86578-86596. https://doi.org/10.1109/ACCESS.2019.2924947

Liu, R., Wang, P., Yan, Z., Lu, X., Wang, M., Yu, J., . . . Ma, X. (2020). Hierarchical classification of pole- like objects in mobile laser scanning point clouds. The Photogrammetry REcord, 35(169). https://doi.org/10.1111/phor.12307

Liu, Z., Li, D., Ge, S. S., & Tian, F. (2020). Small traffic sign detection from large image. Applied Intelligence, 50(1), 1-13. https://doi.org/10.1007/s10489-019-01511-7

Ma, L. (2020). Road Information Extraction from Mobile LiDAR Point Clouds using Deep Neural Networks. In: UWSpace.

Matikainen, L., Lehtomäki, M., Ahokas, E., Hyyppä, J., Karjalainen, M., Jaakkola, A., . . . Heinonen, T. (2016). Remote sensing methods for power line corridor surveys. ISPRS Journal of Photogrammetry and Remote Sensing, 119, 10-31. https://doi.org/10.1016/j.isprsjprs.2016.04.011

Munir, N., Awrangjeb, M., & Stantic, B. (2021, 29 Nov.-1 Dec. 2021). Extraction of Forest Power lines From LiDAR point cloud Data. 2021 Digital Image Computing: Techniques and Applications (DICTA), https://doi.org/10.1109/DICTA52665.2021.9647062

Nguyen, V. N., Jenssen, R., & Roverso, D. (2018). Automatic autonomous vision-based power line inspection: A review of current status and the potential role of deep learning. International Journal of Electrical Power & Energy Systems, 99, 107-120. https://doi.org/10.1016/j.ijepes.2017.12.016

Ortega, S., Trujillo, A., Santana, J. M., Suárez, J. P., & Santana, J. (2019). Characterization and modeling of power line corridor elements from LiDAR point clouds. ISPRS Journal of Photogrammetry and Remote Sensing, 152, 24-33. https://doi.org/10.1016/j.isprsjprs.2019.03.021

Papa, J. P., Falcão, A. X., de Albuquerque, V. H. C., & Tavares, J. M. R. S. (2012). Efficient supervised optimum-path forest classification for large datasets. Pattern Recognition, 45(1), 512-520. https://doi.org/10.1016/j.patcog.2011.07.013

Rastiveis, H., Shams, A., Sarasua, W. A., & Li, J. (2020). Automated extraction of lane markings from mobile LiDAR point clouds based on fuzzy inference. ISPRS Journal of Photogrammetry and Remote Sensing, 160, 149-166. https://doi.org/10.1016/j.isprsjprs.2019.12.009

Shi, Z., Lin, Y., & Li, H. (2020). Extraction of urban power lines and potential hazard analysis from mobile laser scanning point clouds. International Journal of Remote Sensing, 41(9), 3411-3428. https://doi.org/10.1080/01431161.2019.1701726

Shokri, D., Rastiveis, H., Sarasua, W. A., Shams, A., & Homayouni, S. (2021). A Robust and Efficient Method for Power Lines Extraction from Mobile LiDAR Point Clouds. PFG – Journal of Photogrammetry, Remote Sensing and Geoinformation Science. https://doi.org/10.1007/s41064-021-00155-y

Shokri, D., Rastiveis, H., Shams, A., & Sarasua, W. A. (2019). Utility poles extraction from mobile lidar data in urban area based on density information. Int. Arch. Photogramm. Remote Sens. Spatial Inf. Sci., XLII-4/W18, 1001-1007. https://doi.org/10.5194/isprs-archives-XLII-4-W18-1001-2019

Tan, J., Zhao, H., Yang, R., Liu, H., Li, S., & Liu, J. (2021). An Entropy-Weighting Method for Efficient Power-Line Feature Evaluation and Extraction from LiDAR Point Clouds. Remote Sensing, 13(17), 3446. https://www.mdpi.com/2072-4292/13/17/3446

Vishwanathan, S. V. M., & Narasimha Murty, M. (2002, 12-17 May 2002). SSVM: a simple SVM algorithm. Proceedings of the 2002 International Joint Conference on Neural Networks. IJCNN'02 (Cat. No.02CH37290), https://doi.org/10.1109/IJCNN.2002.1007516

Wang, Y., Chen, Q., Liu, L., Zheng, D., Li, C., & Li, K. (2017). Supervised Classification of Power Lines from Airborne LiDAR Data in Urban Areas. Remote Sensing, 9(8). https://doi.org/10.3390/rs9080771

Wang, Y., Chen, Q., Zhu, Q., Liu, L., Li, C., & Zheng, D. (2019). A Survey of Mobile Laser Scanning Applications and Key Techniques over Urban Areas Remote Sensing, 11(13). https://doi.org/10.3390/rs11131540

Wu, J., Tian, Y., Xu, H., Yue, R., Wang, A., & Song, X. (2019). Automatic ground points filtering of roadside LiDAR data using a channel-based filtering algorithm. Optics & Laser Technology, 115, 374-383. https://doi.org/10.1016/j.optlastec.2019.02.039

Wu, Y., Li, Z., Chen, Y., Nai, K., & Yuan, J. (2020). Real-time traffic sign detection and classification towards real traffic scene. Multimedia Tools and Applications. https://doi.org/10.1007/s11042-020-08722-y

Xia, S., Chen, D., Wang, R., Li, J., & Zhang, X. (2020). Geometric Primitives in LiDAR Point Clouds: A Review. IEEE Journal of Selected Topics in Applied Earth Observations and Remote Sensing, 13, 685-707. https://doi.org/10.1109/JSTARS.2020.2969119

Xu, S., Cheng, P., Zhang, Y., & Ding, P. (2015). Error Analysis and Accuracy Assessment of Mobile Laser Scanning System. The Open Automation and Control Systems Journal, 11. https://doi.org/10.2174/1874444301507010485

Yadav, M., & Chousalkar, C. G. (2017). Extraction of power lines using mobile LiDAR data of roadway environment. Remote Sensing Applications: Society and Environment, 8, 258-265. https://doi.org/10.1016/j.rsase.2017.10.007

Yadav, M., Lohani, B., Singh, A. K., & Husain, A. (2016). Identification of pole-like structures from mobile lidar data of complex road environment. International Journal of Remote Sensing, 37(20), 4748-4777. https://doi.org/10.1080/01431161.2016.1219462

Zaboli, M., Rastiveis, H., Shams, A., Hosseiny, B., & Sarasua, W. A. (2019). Classification of mobile terrestrial lidar point cloud in urban area using local descriptors. Int. Arch. Photogramm. Remote Sens. Spatial Inf. Sci., XLII-4/W18, 1117-1122. https://doi.org/10.5194/isprs-archives-XLII-4-W18-1117-2019

Zhang, J., Lin, X., & Ning, X. (2013). SVM-Based Classification of Segmented Airborne LiDAR Point Clouds in Urban Areas. Remote Sensing, 5(8). https://doi.org/10.3390/rs5083749

Zhu, L., & Hyyppä, J. (2014a). Fully-Automated Power Line Extraction from Airborne Laser Scanning Point Clouds in Forest Areas. Remote Sensing, 6(11). https://doi.org/10.3390/rs61111267

Zhu, L., & Hyyppä, J. (2014b). Fully-Automated Power Line Extraction from Airborne Laser Scanning Point Clouds in Forest Areas. Remote Sensing, 6(11), 11267-11282. https://www.mdpi.com/2072-4292/6/11/11267